

In vivo imaging of human *MDR1* transcription in the brain and spine of
MDR1-luciferase reporter mice

Kazuto Yasuda, Cynthia Cline, Yvonne S. Lin, Rachel Scheib, Samit Ganguly,
Ranjit Thirumaran, Amarjit Chaudhry, Richard B. Kim and Erin G. Schuetz

Department of Pharmaceutical Sciences, St. Jude Children's Research Hospital,
Memphis, TN (K.Y., C.C., R.S., S.G., R. T., A.C., E.G.S.), Department of Medicine,
Division of Clinical Pharmacology, University of Western Ontario (R.B.K.), The
University of Iowa College of Pharmacy (M.A.), Department of Pharmaceutics, The
University of Washington (Y.S.L.)

Running Title Page

a) Running Title: Human *MDR1-luc* CNS Reporter Mice

b) Corresponding Author: Erin G. Schuetz, Ph.D., Department of Pharmaceutical Sciences,
St. Jude Children's Research Hospital, 262 Danny Thomas Place, Memphis, TN 38105; PH:
(901) 595-2205; Fax: (901) 595-3125; Email: erin.schuetz@stjude.org

c) Number of text pages: 21

Number of tables: 0 (Supplemental Table 1)

Number of figures: 8

Number of references: 37

Number of words in the Abstract: 243

Number of words in the Introduction: 534

Number of words in the Discussion: 1,412

d) Abbreviations: 1,4-Bis[2(3,5-dichloropyridyloxy)]benzene (TCPOBOP); blood
brain barrier (BBB); multiplex ligation-dependent probe assay (MLPA).

Abstract

P-glycoprotein (the product of the *MDR1* (*ABCB1*) gene) at the blood-brain barrier (BBB) limits CNS entry of many prescribed drugs, contributing to the poor success rate of CNS drug candidates. Modulating Pgp expression could improve drug delivery into the brain but assays to predict regulation of human BBB Pgp are lacking. We developed a transgenic mouse model to monitor human *MDR1* transcription in the brain and spinal cord *in vivo*. A reporter construct consisting of ~10 kb of the human *MDR1* promoter controlling the firefly luciferase gene was used to generate a transgenic mouse line [*MDR1-luc*]. Fluorescence *In Situ* Hybridization localized the *MDR1-luc* transgene on chromosome 3. Reporter gene expression was monitored with an *in vivo* imaging system following D-luciferin injection. Basal expression was detectable in the brain, and treatment with activators of CAR, PXR and the glucocorticoid receptor induced brain and spinal *MDR1-luc* transcription. Since D-luciferin is a substrate of ABCG2, the feasibility of improving D-luciferin brain accumulation (and luciferase signal) was tested by coadministering the dual ABCB1/ABCG2 inhibitor elacridar. The brain and spine *MDR1-luc* signal intensity was increased by elacridar treatment suggesting enhanced D-luciferin brain bioavailability. There was regional heterogeneity in *MDR1* transcription (cortex > cerebellum) that coincided with higher mouse Pgp protein expression. We confirmed luciferase expression in brain vessel endothelial cells by *ex vivo* analysis of tissue luciferase protein expression. We conclude that the *MDR1-luc* mouse provides a unique *in vivo* system to visualize *MDR1* CNS expression and regulation.

Introduction

The drug efflux transporter P-glycoprotein is the product of the *ABCB1/MDR1* gene. Drug transporting P-glycoprotein is a critical part of the blood brain barrier (BBB) and essential in preventing the blood to brain penetration of substrates (Schinkel et al., 1995). However, BBB Pgp also prevents brain delivery of CNS acting drugs including those for brain tumor treatment.

Cranial BBB Pgp is regulated by a number of signaling pathways. In mice the pregnane X receptor (PXR) mediates induction of BBB Pgp by a variety of ligands including the prototypical mouse PXR agonist pregnenolone 16 α -carbonitrile (PCN)). The glucocorticoid receptor has been shown to mediate dexamethasone induction of rodent BBB Pgp (Narang et al., 2008). Activators of the constitutive androstane receptor (CAR), including 1,4-Bis[2(3,5-dichloropyridyloxy)]benzene (TCPOBOP) and phenobarbital induced Pgp protein and function in rat and mouse brain capillaries *ex vivo* (Wang et al., 2010). Spinal BBB Pgp is regulated by activators of the Aryl hydrocarbon receptor (AhR) and Nrf2 (Campos et al., 2012) (Wang et al., 2014).

The human *MDR1* promoter contains PXR and CAR regulatory sequences at about -8 kb (Geick et al., 2001), and human MDR1 transcription can be induced in human liver and intestinal cell models by prototypical PXR and CAR activators (Schuetz et al., 1996a) (Hartley et al., 2004). However, data on regulation of human BBB *MDR1 in vivo* is lacking, despite the fact that there are numerous reasons to understand and predict how *MDR1* is regulated at the human BBB *in vivo* (Miller, 2010). The most extensively described immortalized human BBB cells (hCMEC/D3) (Weksler et al., 2013) maintain a low level of Pgp expression, but have barely detectable expression of PXR and CAR and

failed to show PXR and CAR regulation of *MDR1* (Dauchy et al., 2009). It is unclear whether the cultured cells fail to retain regulation seen *in vivo*, or whether there are differences between rodents and humans in regulation of BBB *MDR1*. Mouse PXR and CAR are expressed in brain and spinal capillaries and regulate mouse Pgp expression (Bauer et al., 2004), and mice humanized with hPXR can similarly regulate mouse BBB Pgp (Miller et al., 2008). However, these models cannot predict the potential of the human *MDR1* 5'-regulatory sequences to respond to these same regulators in the brain *in vivo*.

A mouse *mdr1a-luc* model has previously been generated in which the luciferase reporter was inserted into the genomic locus of the mouse *mdr1a* gene by homologous recombination (Gu et al., 2009) (Gu et al., 2013) and bioluminescent imaging was used to study *in vivo* transcription of the mouse *mdr1a* promoter. However, *mdr1a* transcription was not reported in the *mdr1a-luc* mouse CNS. To gain a better understanding of human *MDR1* regulation, we created a transgenic mouse model with the human *MDR1* promoter driving a luciferase reporter. The *MDR1-luc* mouse demonstrated luciferase signal in the brain and spine that can be used to study in real time *in vivo* transcriptional regulation of the human *MDR1* gene. In addition, we show that treatment of mice with elacridar (an inhibitor of Abcg2/Bcrp at the blood brain barrier) can improve the magnitude of luciferase signal in the brain and spine, presumably by increasing the CNS accumulation of the known Bcrp substrate D-luciferin.

Materials and Methods

Materials. TCPOBOP, elacridar, rifampin and dexamethasone were purchased from Sigma (St. Louis, MO) and sodium phenobarbital from J.T. Baker Inc. (Phillipsburg, NJ).

Animals. FVB mice were purchased from Taconic Farms (Germantown, NY). All experimental procedures were approved by the Institutional Animal Care and Use Committee of St Jude Children's Research Hospital in accordance with US National Institutes of Health guidelines.

Creation of *MDR1-luc* transgenic mice. The human *MDR1-luciferase* plasmid was generated by amplifying the human *MDR1* promoter (- 9,912/+180, relative to the transcription initiation site) and ligating it into the *KpnI/SmaI* site of pGL3Basic (Promega, Madison, WI) as described (Schuetz et al., 2002). The transgene was linearized by restriction enzyme digestion and the purified fragment was microinjected into single cell-stage FVB embryos and implanted into pseudo-pregnant mice.

***MDR1-luc* genotyping.** Genomic DNA was isolated from mouse tails using the DNeasy Blood and Tissue Kit (Qiagen, Valencia, CA). Two methods were used to determine the presence or absence of luciferase in genomic DNA. Luciferase (255 bp fragment) was PCR amplified using primers lucS (TTCGCAGCCTACCGTGGTGTT) and lucAS (GGCAGACCAGTAGATCCAGAG) and HotMaster *Taq* DNA polymerase (5 Prime Inc., Gaithersburg, MD). PCR conditions included an initial denaturation (94°C for 2 min),

followed by 32 cycles of denaturation (94°C for 20s), annealing (55°C for 20s), and synthesis (65°C for 30s), and a final synthesis (65°C for 1min). The amplicon was visualized on a 2% agarose gel. Alternatively, mice were genotyped using real time PCR with specific probes designed to detect luciferase (Transnetyx, Cordova, TN). Insertion of the entire *MDR1* promoter was confirmed by PCR amplification using genomic DNA from *MDR1-luc* mice and eight sets of human *MDR1* specific primers that specifically amplified regions between -9447 bp to +180bp of the human *MDR1* promoter transgene.

Multiplex ligation-dependent probe assay (MLPA) to genotype zygosity of *MDR1-luc* transgene alleles.

Since the exact insertion site of the *MDR1-luc* transgene was not known, MLPA was used to genotype transgene zygosity. During MLPA, an oligonucleotide ligation reaction was performed, followed by PCR using fluorescein-conjugated primer, such that the amount of PCR product generated for each genomic sequence is directly proportional to the number of input copies. The mice bearing *Luc* transgene alleles were analyzed by designing our own MLPA *Luc* probe set to have an amplification product of size 140 bp. Three control probes elsewhere in the mouse genome were used, with amplification products ranging in size from 108bp, 114bp and 136 bp (Kozlowski et al., 2007). Each probe set was composed of a 5' and a 3' half-probe, each containing unique target specific sequence, stuffer sequence, and universal primer sequences on their 5' and 3' ends, (Kozlowski et al., 2007). All probes were synthesized at 25N scale and purified by polyacrylamide gel electrophoresis (Invitrogen Life Technologies, USA). 3' half-probes were synthesized with a 5' phosphate to facilitate ligation.

MLPA reaction. All reagents except probe mixes were from MRC-Holland (Amsterdam, The Netherlands) and reactions performed according to manufacturers' protocol. MLPA was performed by incubating 50 ng (10 ng/μL using DNA suspension buffer (Cat No. T0221 from TEKnova, USA)) of mouse tail genomic DNA in 5 μL at 98°C for 5 min; cooling to room temperature, mixing with 1.5 μL of *Luc* transgene specific probe mixture (containing 1.5 fmol each probe) and 1.5 μL SALSA hybridization buffer, denaturing (95°C for 2 min), and hybridizing (60°C for 16 hours). Hybridized probes were then ligated at 54°C for 15 min by addition of 32 μL ligation mixture. Following heat inactivation, 40 μL ligation reaction was mixed with 10 μL PCR mixture (SALSA polymerase, dNTPs, and universal primers, one of which was labeled with fluorescein), and subjected to PCR (35 cycles). Amplification products were diluted in water (1:10) and then 1:9 in Hi-Di™ formamide (Applied Biosystems, USA) containing 1/36 volume of GeneScan 500 LIZ size standard (Applied Biosystems), to a final dilution of 20 to 200 fold, and then were separated by size on an 3730XL DNA Analyzer (Applied Biosystems / Life Technologies). Electropherograms were analyzed by GeneMapper® v5 (Applied Biosystems), and peak height data were exported to an Excel table. Normalization of peak height data was done by dividing each *Luc* transgene peak height by the average signal from three control probes, followed by division by a similar value calculated from a set of reference samples known to be heterozygotes for the transgene allele. This ratio reflects the copy number of *Luc* transgene.

MLPA *Luc* Probe Set for Mouse Transgene: 5' Half-Probe (75nt) [5' Universal Prime, GGGTTCCTAAGGGTTGGA (19nt); 5' Stuffer, cgctactact (10nt), 5' Target, AATTGGAATCCATCTTGCTCCAACACCCCAACATCTTCGACGCAGG (46nt)] and

3' Half- Probe (65nt) [3'Target, TGTCGCAGGTCTTCCCGACGATGACGCCGGTGA ACTT (37nt); 3'Stuffer, gacca (5nt); 3'Universal Primer, TCTAGATTGGATCTTGCTGGCGC (23nt)] with a total product length of 140bp. Control probe sets were used exactly as indicated (Kozlowski et al., 2007). The probe set consists of a 5' half-probe and a 3' half-probe. Each probe contains universal primer sequence, stuffer sequence, and target sequence, the latter of which is specific for the transgene being assessed. Total length of PCR product assessed by capillary electrophoresis is shown by the total product length. Primers used for PCR: SALSA Forward primer (Labeled): *GGGTTCCCTAAGGGTTGGA. SALSA Reverse primer (Unlabeled): GTGCCAGCAAGATCCAATCTAGA

***MDR1-luc* transgene localization by fluorescence in situ hybridization (FISH).** The purified *MDR1-luc* plasmid was labeled with digoxigenin-¹¹dUTP (Roche Molecular Biochemicals, Indianapolis, IN) by nick translation, combined with sheared mouse DNA and a biotinylated chromosome 3 centromere-specific probe (Oncor, Gaithersburg, MD) and hybridized to metaphase chromosomes derived from the lungs of two heterozygous *MDR1-luc* transgenic mice in a solution containing 50% formamide, 10% dextran sulfate, and 2 x SSC. Probes were detected by incubating the slide in fluorescein-labeled anti-digoxigenin antiserum for the *MDR1-luc* transgene (green) and a biotin labeled centromeric control probe for chromosome 3 (red) (Roche Molecular Biochemicals). The chromosomes were then stained with 4, 6-diamidino-2-phenylindole (DAPI) and analyzed. In order to determine a band assignment for the transgene insertion sites, measurements were made of the specifically hybridized chromosome to determine the position of the transgene relative to the

heterochromatic-euchromatic boundary and the telomere of the specifically hybridizing chromosome. The *MDR1-luc* mice were found to have a transgene insertion that is 10% of the distance from the heterochromatic-euchromatic boundary to the telomere of chromosome 3, an area that corresponds to band 3A to 3B.

***In Vivo* bioluminescent imaging of *MDR1-luc* reporter mice.** Mice were anesthetized by isoflurane gas (2%, inhalation) and given an i.p. injection of D-firefly luciferin (240 mg/kg) (Gold Biotechnology, St. Louis, MO). Mice were placed into the chamber of Xenogen IVIS 200 imaging system and bioluminescence images were obtained under isoflurane anesthesia using 1 min exposures beginning 10 min after D-luciferin injection (<http://www.xenogen.com/demo4.html>). The images were quantitatively analyzed by Living Image® version 4.3.1 image analysis software (Caliper Life Sciences, Hopkinton, MA). Total bioluminescence measurements (photon/second) were quantified over a contour drawn around a brain and coronal slices. Results were repeated two to three times in independent animals. All *in vivo* images are scaled to maximum intensity of 1×10^5 photons (p)/s/cm²/sr.

***MDR1-luc* mice drug treatments.** Female *MDR1-luc* transgenic mice (8-12 weeks) (n=3-5/group) were treated with drugs that were selected based on clinical relevance and previous data demonstrating that the drugs are prototypical Pgp inducers (Supplemental Methods and Supplemental Table 1). Some mice were treated by oral gavage with elacridar (100 mg/kg) suspension (prepared in 0.5% methocel® 60 HG (Sigma, St. Louis, MO) and 1% Tween 80 (Sigma) to obtain a 10 mg/ml formulation) the final four hours before *in vivo* imaging.

***Ex Vivo* imaging of bioluminescence in brain slices from *MDRI-luc* transgenic mice.**

After *in vivo* imaging, mice were immediately sacrificed under anesthesia by carbon dioxide gas following cervical dislocation. Whole brain was immediately dissected out of the skull and dorsal and ventral of brain image were taken. The brain was immobilized on a brain slicer matrix (Zivic Instruments, Pittsburgh, PA) and coronally sliced into 2mm thickness. The brain slices were placed into individual wells of a 12 well plate. D-luciferin was directly re-applied on each brain slice and coronal image was taken from both sides of the slices. Dorsal, ventral, sagittal and coronal images were scaled to maximum intensity of 1×10^5 photons (p)/s/cm²/sr while microdissected brain images were scaled to maximum intensity of 3.5×10^4 photons (p)/s/cm²/sr.

Quantitation of fluorescently immunostained mouse Pgp and CD31 in coronal brain slices. *MDRI-luc* adult mice were perfused with cold PBS and 4% paraformaldehyde (PFA), the brains were removed and processed for paraffin embedding. Embedded tissue was cut at 4μm thickness. Slides were deparaffinized and antigens retrieved with Target Retrieval solution pH 6.0 (Dako #S1699, Carpinteria, California) in a pressure cooker for 15 minutes. After retrieval, slides were rinsed, treated with 3% hydrogen peroxide, and blocked with 3% Normal Donkey serum (Jackson ImmunoResearch #017-000-121, West Grove, PA) in Phosphate Buffered Saline with 0.3% Triton X-100 (PBST). Slides were incubated with purified rabbit anti-Pgp antibody (1:50,000) (raised to a peptide containing amino acids 555-575 of human Pgp and prepared by Dr. John Schuetz) and goat anti CD31 IgG (1:300) (R&D Systems #AF3628, Minneapolis, MN) for 1 hr. Stained slides were rinsed three times in PBST and then incubated with Alexa donkey

anti-rabbit 568 (A10042) or Alexa donkey anti-goat 488 (A11055) secondary antibody (Life Technologies, Grand Island, NY) at 1:500 for 1 hour and coverslipped with Permount (Fisher #SP15-500) (ThermoFisher Scientific, Waltham, MA).

Imaging was performed on a widefield Nikon TE2000S microscope equipped with a 20X 0.75NA Plan Apo lens and a Photometrics Coolsnap K4 camera. Fluorescent images were captured by using 3 X 3 binning and cropping to the center of the chip, resulting in individual images that were 512 x 512 pixels. Images were captured as montages and were typically comprised of 1000-1300 images. Quantitation was performed using NIS Elements software. Each channel was thresholded to distinguish signal above background and mean intensities for each thresholded channel were calculated. In total 18 measurements of 39,992 μm^2 size (the region of interest, ROI) were randomly selected per region and taken for both frontal cortex and cerebellum. Numerical values were determined for binary area (total area of pixels that show any intensity within the threshold for the ROI (and this could be bright or dim)); Binary sum (total intensity within the set threshold); and, Binary mean intensity (sum intensity/binary area). To determine differences in vessel density in each region, the binary area for CD31 in the frontal cortex vs. cerebellum was compared. To determine the expression of Pgp per brain capillary in each region we calculated the mean Pgp intensity/mean CD31 intensity for the frontal cortex vs. cerebellum.

All statistical calculations were performed using statistical program R: A Language and Environment for Statistical Analysis (<http://www.R-project.org>). Group differences were analyzed nonparametrically using the Wilcoxon rank-sum test to compare the mean intensity of Pgp (normalized to mean intensity of CD31) for each

square between the frontal cortex and cerebellum.

Colorimetric Immunostaining of Luciferase in Mouse Brain. Adult mice (*MDR1-luc* and FVB controls) were perfused with cold PBS and 4% PFA, brains were removed and processed for paraffin embedding. Embedded tissue was cut at 4 μ m thickness. These slides were deparaffinized and antigens were retrieved with Target Retrieval solution pH 6 (Dako #S1699, Carpinteria, California) in a pressure cooker for 15 minutes. After retrieval, slides were rinsed, treated with 3% hydrogen peroxide, and blocked with Background Sniper (BS966H, Biocare Medical, Concord, CA) followed by primary antibody staining with rabbit anti-luciferase IgG (1:1000, sc-32896, Santa Cruz Biotechnology, Dallas, Texas) or rabbit IgG isotype control antibody (Abcam #ab27478) in a humidified chamber overnight at 4°C. Stained slides were rinsed three times in PBST (0.3% Triton X-100) then incubated with Rabbit-on-Rodent HRP-Polymer secondary (#RMR622H, Biocare Medical, Concord, CA). Slides were rinsed three times in PBST then color detection was completed by the use of diaminobenzidine (DAB; #TA-125-HDX, ThermoFisher Scientific, Waltham, MA) and counterstained with diluted hematoxylin (1:7 dilution, #TA-125-MH, ThermoFisher Scientific, Waltham, MA). Slides were then dehydrated and coverslipped with Permount (#SP15-500, ThermoFisher Scientific, Waltham, MA). Light microscopy was performed at 60X on a Nikon microscope.

Results

***MDR1-luc* transgenic mice.** We developed *MDR1-luc* mouse lines containing ~10 kb of 5'-flanking human *MDR1* sequence directing expression of luciferase (Fig 1A). After zygote microinjection and implantation, we identified multiple founder lines based on PCR screening and mouse tail luminescence. Two founder lines showed luciferase expression in brain and spine and one of these transgenic lines was selected for this study. We performed fluorescence *in situ* hybridization (FISH) analysis of *MDR1-luc* in heterozygous transgenic mice. The *MDR1-luc* mice had insertion of the transgene at a single location on chromosome 3 (Fig 1B) and it was observed in all metaphase spreads examined from this line. PCR analysis of genomic DNA from the transgenic line with primers covering 9766 bp of the human *MDR1* promoter confirmed that the entire promoter had inserted into the mouse genome.

***MDR1-luc* is inducible in the head and spine of reporter mice by activators of CAR, PXR and GCR and the Bcrp/Abcg2 inhibitor, elacridar, further increases brain bioluminescence.** *In vivo* dorsal and ventral imaging of transgenic mice showed that the highest basal level of luciferase activity was in the head region and in some mice along the spine (Fig 2). The *MDR1-luc* construct contains the regulatory cluster of nuclear response elements (-7864 to -7817bp relative to the transcription start site of the human *MDR1* gene) (Geick et al., 2001). Since P-glycoprotein is induced at the blood brain barrier by CAR activators (Bauer et al., 2004), mice were treated with the potent CAR

agonist TCPOBOP (Tzameli et al., 2000). Relative to baseline luciferase activity, there was a time-dependent induction of luminescence in the brain and spine. This pattern demonstrated that the human *MDR1* 5'-flanking sequence was sufficient to direct CNS expression of the luciferase reporter.

We next tested whether human *MDR1* transcription was induced by other drugs demonstrated to increase Pgp in the brains of mice *in vivo* (Bauer et al., 2004) (Narang et al., 2008). Treatment with phenobarbital (CAR activator) and dexamethasone (glucocorticoid receptor & PXR activator), each increased *MDR1-LUC* transcription in brains of the transgenic mice (Fig 3). Since D-luciferin is a substrate of Bcrp (Zhang et al., 2007), a transporter that can limit brain availability of D-luciferin at the blood brain barrier (Bakhsheshian et al., 2013), we treated mice with an oral dose of elacridar (100 mg/kg) for four hours to maximize the brain to plasma concentration (Sane et al., 2012). Elacridar increased the total *MDR1-luc* bioluminescent signal up to two-fold in vehicle and drug treated mice (Fig 4), but did not change the regional pattern of *MDR1-luc* expression in the brain and spine of any mice. Elacridar's effect appears to be due to inhibition of Bcrp, and not induction of Pgp, because four hour treatment with elacridar failed to activate PXR and increase Pgp in an *in vitro* test system (E. Schuetz unpublished observation).

Brain localization of the human *MDR1-luc* signal versus mouse P-glycoprotein by IHC. Brains from the *MDR1-luc* mice imaged *in vivo* were excised and imaged dorsally, ventrally, sagittally (Fig 4) and in serial coronal slices (Fig 5) to further localize regional distribution of *MDR1-luc* bioluminescence. The luciferase distribution pattern

was unique in the *MDR1*-luc model compared with other transgenic reporter mice such as androgen receptor element (ARE)-luc mice (Dart et al., 2013), or estrogen receptor element (ERE)-luc mice (Stell A et al., 2008), or tyrosine hydroxylase promoter-luc mice (Dodd KW et al., 2011). While the intensity of *MDR1* transcription increased with various inducers, the distribution pattern of luciferase signal throughout the brain was similar, regardless of inducer. All chemicals increased *MDR1* transcription to a greater extent in the cortex compared to the cerebellum. The coronal slices were further dissected and luciferase signal was higher in the cortex vs. cerebellum and was expressed in the white matter, thalamus, striatum, hippocampus, substantia nigra, brain stem and internal capsule (Fig 6).

Brain tissue was processed for colorimetric immunohistochemistry using an anti-luciferase antibody. The luciferase signal was localized to the BBB of vehicle treated *MDR1*-luc mice, and was induced in the endothelial cells of capillaries of phenobarbital treated *MDR1*-luc mice (Fig 7).

To determine whether mouse Pgp showed a similar regional pattern of brain expression in these same mice, *MDR1*-luc brain tissue was processed by fluorescent immunohistochemistry using anti-Pgp and anti-CD31 (a vessel endothelial specific marker) antibodies and the fluorescent signal intensity was quantified. Consistent with the regional variation in *MDR1*-luc transcription, the mean mouse BBB Pgp signal, normalized to CD31 signal, was higher in the frontal cortex compared to the cerebellum (Fig 8). Regional differences in mouse brain local blood flow rates, brain capillary density, perfusion rate, and Pgp activity have been reported. Local cerebral blood flow was reported to be 1.65 to 1.82-fold greater in regions of brain cortex vs. cerebellum

(Otsuka et al., 1991) (Zhao and Pollack, 2009). Thus, the regional differences in MDR1-luc reporter activity documented by photon imaging appear to mirror regional differences reported in blood flow, capillary density and Pgp expression (Fig 8).

Discussion

A transgenic mouse was developed containing ~10 kb of the 5'-regulatory region of human *MDR1* driving a luciferase reporter in FVB mice in order to study regulation of human BBB *MDR1*. This humanized model allowed real-time monitoring of *MDR1* transcriptional activity throughout the mouse brain using the luciferase reporter, repeated measurements on the same animal (as opposed to sacrifice at specific time points), rapid detection of perturbations to gene expression and characterization of the *in vivo* response. *MDR1* brain and spine transcription increased following treatment with PXR, CAR and GCR activators. *Ex vivo* luciferase immunostaining of brain tissue confirmed that *MDR1* transcriptional activity was localized to vessel capillary endothelial cells. Thus, the *MDR1*-luc mouse offers an *in vivo* model to non-invasively monitor MDR1 regulation, both quantitatively and spatially.

This study also confirmed that a Bcrp inhibitor could enhance optimal imaging of a luciferase reporter gene in mouse brain, presumably by enhancing D-luciferin brain bioavailability. The brain penetration of ^{14}C -D-luciferin in mice was previously shown to be very low (Berger et al., 2008) consistent with the finding that luciferin is a Bcrp substrate (Zhang et al., 2007). Indeed, treatment with Bcrp inhibitors enhanced D-luciferin brain penetration of a low dose of D-luciferin (18 mg/kg) (Bakhsheshian et al., 2013) suggesting BBB Bcrp can limit brain availability of D-luciferin. At the D-luciferin concentrations used in most studies (and this one) (i.p. 240 mg/kg) luciferin can clearly penetrate the BBB as evidenced by *MDR1-luc* brain signals even without a Bcrp blocker. However, oral elacridar pretreatment enhanced the brain

luminescence suggesting BBB Bcrp still limits some D-luciferin brain penetration, even at the high doses used here.

Our data shows that the *MDR1-luc* signal was not uniformly distributed in mouse brain and was consistently higher in the cortex vs. cerebellum in both untreated and treated mice. In addition, quantitative immunohistochemistry analysis found the mean Pgp expression in mouse brain was significantly higher in cortex compared to cerebellum (Fig 8). These results are consistent with several lines of evidence that Pgp *activity* shows regional distribution in the brain. First, Zhao and Pollack (Zhao and Pollack, 2009) previously performed *in situ* brain perfusion of Pgp substrates in Pgp WT and KO mice and found that the rate of regional perfusion flow and Pgp efflux activity was directly proportional to local capillary density in mouse brain. For example, pons, medulla and cerebellum had the lowest vascular volume and functional flow rate, lowest blood perfusion flow rate, and lowest Pgp efflux ratio. Conversely, colliculi, thalamus and parietal cortex had the highest vascular volume and functional flow rate and the highest Pgp efflux ratio. Secondly, some animal studies with PET imaging have reported that Pgp inhibition increases substrate penetration to the greatest extent in the cerebellum (Zoghbi et al., 2008) and least in the frontal cortex. This result is interpreted to mean that Pgp function is lower in cerebellum vs. cortex and this results in a greater effect of the Pgp inhibitor on Pgp function in the cerebellum vs. the cortex. Hence, the regionality of *MDR1-luc* expression is consistent with literature reports on regionality in Pgp-mediated efflux, and also has potential pharmacological implications, for example, since opioid receptors (targets of Pgp opioid substrates) are also concentrated in the thalamus and cortex regions (Inturrisi, 2002).

We recognize that the regional patterns of *MDR1-luc* activity may not simply be due to heterogeneity in its expression. First, Regional blood flow differences would also result in regional differences in local D-luciferin substrate delivery/distribution and this could very well affect luminescence intensity. Hence, the brain regions with the largest vascular volume (cortex > cerebellum) would correspondingly have the highest perfusion concentration of D-luciferin. Thus, the heterogeneity in Pgp expression could be due both to the local capillary density (cortex> cerebellum) equaling higher expression level of Pgp, and to the higher blood flow and delivery/exposure of D-luciferin. Similarly, we cannot confirm that the *MDR1* induction potential is not affected by distribution of chemicals at the site of induction, because we did not measure regional concentration of each inducer. However, since co-treatment with the Pgp/Bcrp dual inhibitor elacridar + Pgp substrates did not change the distribution pattern of *MDR1-luc* signal for any of the drugs (only magnitude of induction), it suggests the luciferase distribution pattern reflects regional differences in *MDR1* transcription.

Understanding whether a drug is an inducer of human *MDR1* is important for predicting drug-drug interactions. The pharmacodynamic consequence of inducing BBB Pgp is predicted to be tightening of the BBB drug barrier (Miller et al., 2008), and decreased brain exposure to Pgp substrates. Although induction of Pgp has been shown in the brains of some animal models following drug or chemical treatment, there is currently no *in vivo* model to predict induction of human *MDR1* transcription in brain. Equally important, because the *in vitro* Pgp induction models are not well understood the current FDA guidance on evaluating Pgp induction potential of a new

chemical entity is based not on direct evaluation of whether a drug induces Pgp, but on whether it induces CYP3A (Zhang et al., 2009). If the drug is a CYP3A inducer, then further testing for Pgp induction *in vivo* is warranted. However, this advice is complicated by examples of tissue and species differences in induction of CYP3A and *MDR1* (Schuetz et al., 1996a) (Hartley et al., 2004). Moreover, the human BBB cells culture model has lost MDR1 regulation (Dauchy et al., 2009). In addition, it is desirable to determine if induction of Pgp actually occurs in the brain *in vivo* because of the added complication that the inducer has to effectively penetrate the BBB drug transport barrier. Indeed, rifampin, phenobarbital and dexamethasone are all reported Pgp substrates (Schuetz et al., 1996b)(Luna-Tortos et al., 2008)(Schinkel et al., 1995). Nevertheless, at the drug exposure levels used in these studies, each of these drugs was clearly able to sufficiently penetrate the brain endothelial cells to induce MDR1. Hence, an *in vivo* model was clearly needed for further assessment of *MDR1* regulation in the brain *in vivo*.

It is important to understand regulation of *MDR1* because basic mechanistic understanding of how brain Pgp is regulated by drugs, inflammation and oxidative stress and in disease states is lacking (Miller, 2010). Ex vivo analysis of Pgp in rodent brain tissue found that BBB Pgp is induced by seizures (van Vliet et al., 2007), and in amyotrophic lateral sclerosis (Jablonski et al., 2012), and that phenobarbital induced Pgp only in the hippocampus of epileptic rats (van Vliet et al., 2007) (a phenobarbital induction pattern strikingly different from what we observed in *MDR1-luc* mice). *MDR1-luc* mice would permit *in vivo* analysis of the temporal effects of these disease state and their treatments on regional human *MDR1* transcription. Understanding whether human *MDR1-luc* could be induced *in vivo* is also of potential interest in modulation of

Alzheimer's disease. It was previously shown that Pgp could efflux amyloid beta (A β) peptide from the brain (Cirrito et al., 2005), and hence, that modulation of Pgp activity might directly influence progression of A β pathology. Our results demonstrate that brain Pgp can be induced by a variety of drugs including rifampin which, intriguingly, has previously been shown to slow the decline of patients with mild to moderate Alzheimer's (Loeb et al., 2004), potentially through induction of *MDR1*.

***MDR1-luc* mice might be of value to identify chemicals that down-regulate *MDR1* transcription at the BBB and enhance brain exposure of Pgp substrates.**

Attempts to block BBB Pgp and enhance drug brain delivery have been largely unsuccessful, making different approaches, such as modulating Pgp expression, important alternative strategies (Miller, 2010). Indeed there has been limited success in inhibiting BBB Pgp efflux in humans, primarily due to the inability to achieve unbound systemic inhibitor concentrations sufficient to elicit appreciable inhibition (Kalvass et al., 2013). Although not tested in this study, one alternative approach would be to screen chemical libraries to identify chemicals capable of down regulating *MDR-luc* transcription *in vitro*; in theory, these chemicals could be rapidly evaluated for their potential to regulate expression of brain *MDR1-luc* in whole animals.

The application of this *MDR1-luc* model to predict regulation of human Pgp still has challenges including species differences in the interaction of compounds with mouse vs. human PXR, and in pathways of metabolism or BBB transport of drugs. However, interbreeding the *MDR1-luc* model with mice humanized for nuclear hormone receptors, CYPs or drug transporters (Scheer & Wolf, 2013)(Scheer & Wolf, 2014) would potentially improve the utility and predictability of this *in vivo* model.

Acknowledgements

We thank Dr. Balasubramanian Poonkuzhali for PCR analysis of the *MDR1* promoter in genomic DNA from the *MDR1-luc* transgenic line, Dr. Lubin Lan for some of the *MDR1-luc* imaging, Dr. Michael Taylor's lab for stereoscope assistance, and Dr. Richard Smeyne's laboratory for mouse brain microdissection assistance. We thank the following St Jude Children's Research Hospital shared resource facilities for expert technical assistance: The Transgenic Animal Core (Dr. John Raucci), the Animal Imaging Center (Cheryl Winters), the Cell and Tissue Imaging Center (Dr. Victoria Frohlich and Jennifer Peters); and the Cancer Center Core Cytogenetics laboratory (Dr. Jill Lahti) for FISH analysis.

Authorship Contributions

Participated in research design: Schuetz, Yasuda, Cline

Conducted experiments: Yasuda, Cline, Lin, Scheib

Contributed new reagents or analytic tools: Thirumaran, Kim

Performed data analysis: Schuetz, Yasuda, Cline, Chaudhry

Wrote or contributed to the writing of the manuscript: Schuetz, Yasuda, Cline, Scheib,

Ganguly, Thirumaran

References

Bakhsheshian, J, Wei, BR, Chang, KE, Shukla, S, Ambudkar, SV, Simpson, RM, Gottesman, MM and Hall, MD (2013) Bioluminescent imaging of drug efflux at the blood-brain barrier mediated by the transporter ABCG2. *Proc Natl Acad Sci U S A* **110**: 20801-20806.

Bauer, B, Hartz, AM, Fricker, G and Miller, DS (2004) Pregnane X receptor up-regulation of P-glycoprotein expression and transport function at the blood-brain barrier. *Mol Pharmacol* **66**: 413-419.

Berger, F, Paulmurugan, R, Bhaumik, S and Gambhir, SS (2008) Uptake kinetics and biodistribution of ¹⁴C-D-luciferin--a radiolabeled substrate for the firefly luciferase catalyzed bioluminescence reaction: impact on bioluminescence based reporter gene imaging. *Eur J Nucl Med Mol Imaging* **35**: 2275-2285.

Campos, CR, Schroter, C, Wang, X and Miller, DS (2012) ABC transporter function and regulation at the blood-spinal cord barrier. *J Cereb Blood Flow Metab* **32**: 1559-1566.

Cirrito, JR, Deane, R, Fagan, AM, Spinner, ML, Parsadanian, M, Finn, MB, Jiang, H, Prior, JL, Sagare, A, Bales, KR, Paul, SM, Zlokovic, BV, Piwnicka-Worms, D and Holtzman, DM (2005) P-glycoprotein deficiency at the blood-brain barrier increases

amyloid-beta deposition in an Alzheimer disease mouse model. *J Clin Invest* **115**: 3285-3290.

Dart DA, Waxman J, Aboagye EO, Bevan CL (2013) Visualising androgen receptor activity in male and female mice. *PLOS ONE* **8**:e71694

Dauchy, S, Miller, F, Couraud, PO, Weaver, RJ, Weksler, B, Romero, IA, Scherrmann, JM, De Waziers, I and Decleves, X (2009) Expression and transcriptional regulation of ABC transporters and cytochromes P450 in hCMEC/D3 human cerebral microvascular endothelial cells. *Biochem Pharmacol* **77**: 897-909.

Dodd KW, Burns TC, Wiesner SM, Kudishevich E, Schomberg DT, Jung BW, Kim, JE, Ohlfest JR, Low WC (2011) Transgenic mice expressing luciferase under a 4.5 kb Tyrosine Hydroxylase promoter. *Cureus* **3**:e34.

Geick, A, Eichelbaum, M and Burk, O (2001) Nuclear receptor response elements mediate induction of intestinal MDR1 by rifampin. *J Biol Chem* **276**: 14581-14587.

Gu, L, Chen, J, Synold, TW, Forman, BM and Kane, SE (2013) Bioimaging real-time PXR-dependent *mdr1a* gene regulation in *mdr1a*.fLUC reporter mice. *J Pharmacol Exp Ther* **345**: 438-445.

Gu, L, Tsark, WM, Brown, DA, Blanchard, S, Synold, TW and Kane, SE (2009) A new model for studying tissue-specific *mdr1a* gene expression in vivo by live imaging. *Proc Natl Acad Sci U S A* **106**: 5394-5399.

Hartley, DP, Dai, X, He, YD, Carlini, EJ, Wang, B, Huskey, SE, Ulrich, RG, Rushmore, TH, Evers, R and Evans, DC (2004) Activators of the rat pregnane X receptor differentially modulate hepatic and intestinal gene expression. *Mol Pharmacol* **65**: 1159-1171.

Inturrisi, CE (2002) Clinical pharmacology of opioids for pain. *Clin J Pain* **18**: S3-13.

Jablonski, MR, Jacob, DA, Campos, C, Miller, DS, Maragakis, NJ, Pasinelli, P and Trotti, D (2012) Selective increase of two ABC drug efflux transporters at the blood-spinal cord barrier suggests induced pharmacoresistance in ALS. *Neurobiol Dis* **47**: 194-200.

Kalvass, JC, Polli, JW, Bourdet, DL, Feng, B, Huang, SM, Liu, X, Smith, QR, Zhang, LK, Zamek-Gliszczyński, MJ and International Transporter, C (2013) Why clinical modulation of efflux transport at the human blood-brain barrier is unlikely: the ITC evidence-based position. *Clin Pharmacol Ther* **94**: 80-94.

Kozłowski, P, Lin, M, Meikle, L and Kwiatkowski, DJ (2007) Robust method for distinguishing heterozygous from homozygous transgenic alleles by multiplex ligation-dependent probe assay. *Biotechniques* **42**: 584-588.

Loeb, MB, Molloy, DW, Smieja, M, Standish, T, Goldsmith, CH, Mahony, J, Smith, S, Borrie, M, Decoteau, E, Davidson, W, McDougall, A, Gnarp, J, O'D, OM and Chernesky, M (2004) A randomized, controlled trial of doxycycline and rifampin for patients with Alzheimer's disease. *J Am Geriatr Soc* **52**: 381-387.

Luna-Tortos C, Fedrowitz M, Loscher W (2008) Several major antiepileptic drugs are substrates for human P-glycoprotein. *Neuropharmacology* **55**:1364-1375.

Miller, DS (2010) Regulation of P-glycoprotein and other ABC drug transporters at the blood-brain barrier. *Trends Pharmacol Sci* **31**: 246-254.

Miller, DS, Bauer, B and Hartz, AM (2008) Modulation of P-glycoprotein at the blood-brain barrier: opportunities to improve central nervous system pharmacotherapy. *Pharmacol Rev* **60**: 196-209.

Narang, VS, Fraga, C, Kumar, N, Shen, J, Throm, S, Stewart, CF and Waters, CM (2008) Dexamethasone increases expression and activity of multidrug resistance transporters at the rat blood-brain barrier. *Am J Physiol Cell Physiol* **295**: C440-450.

Otsuka, T, Wei, L, Acuff, VR, Shimizu, A, Pettigrew, KD, Patlak, CS and Fenstermacher, JD (1991) Variation in local cerebral blood flow response to high-dose pentobarbital sodium in the rat. *Am J Physiol* **261**: H110-120.

Sane, R, Agarwal, S and Elmquist, WF (2012) Brain distribution and bioavailability of elacridar after different routes of administration in the mouse. *Drug Metab Dispos* **40**: 1612-1619.

Scheer N and Wolf CR (2013) Xenobiotic receptor humanized mice and their utility. *Drug Metab Rev* **45**: 110-121.

Scheer N and Wolf CR (2014) Genetically humanized mouse models of drug metabolizing enzymes and transporters and their applications. *Xenobiotica* **44**: 96-108.

Schinkel, AH, Wagenaar, E, van Deemter, L, Mol, CA and Borst, P (1995) Absence of the mdr1a P-Glycoprotein in mice affects tissue distribution and pharmacokinetics of dexamethasone, digoxin, and cyclosporin A. *J Clin Invest* **96**: 1698-1705.

Schuetz, E, Lan, L, Yasuda, K, Kim, R, Kocarek, TA, Schuetz, J and Strom, S (2002) Development of a real-time in vivo transcription assay: application reveals pregnane X receptor-mediated induction of CYP3A4 by cancer chemotherapeutic agents. *Mol Pharmacol* **62**: 439-445.

Schuetz, EG, Beck, WT and Schuetz, JD (1996a) Modulators and substrates of P-glycoprotein and cytochrome P4503A coordinately up-regulate these proteins in human colon carcinoma cells. *Mol Pharmacol* **49**: 311-318.

Schuetz, EG, Schinkel, AH, Relling, MV and Schuetz, JD (1996b) P-glycoprotein: a major determinant of rifampicin-inducible expression of cytochrome P4503A in mice and humans. *Proc Natl Acad Sci U S A* **93**: 4001-4005.

Stell A, Belcredito S, Ciana P, Maggi A (2008) Molecular imaging provides novel insights on estrogen receptor activity in mouse brain. *Mol Imaging* **7**:283-292.

Tzamelis, I, Pissios, P, Schuetz, EG and Moore, DD (2000) The xenobiotic compound 1,4-bis[2-(3,5-dichloropyridyloxy)]benzene is an agonist ligand for the nuclear receptor CAR. *Mol Cell Biol* **20**: 2951-2958.

Wang, X, Campos, CR, Peart, JC, Smith, LK, Boni, JL, Cannon, RE and Miller, DS (2014) Nrf2 upregulates ATP binding cassette transporter expression and activity at the blood-brain and blood-spinal cord barriers. *J Neurosci* **34**: 8585-8593.

Wang, X, Sykes, DB and Miller, DS (2010) Constitutive androstane receptor-mediated up-regulation of ATP-driven xenobiotic efflux transporters at the blood-brain barrier. *Mol Pharmacol* **78**: 376-383.

Weksler, B, Romero, IA and Couraud, PO (2013) The hCMEC/D3 cell line as a model of the human blood brain barrier. *Fluids Barriers CNS* **10**: 16.

Zhang, L, Zhang, YD, Zhao, P and Huang, SM (2009) Predicting drug-drug interactions: an FDA perspective. *AAPS J* **11**: 300-306.

Zhang, Y, Bressler, JP, Neal, J, Lal, B, Bhang, HE, Laterra, J and Pomper, MG (2007) ABCG2/BCRP expression modulates D-Luciferin based bioluminescence imaging. *Cancer Res* **67**: 9389-9397.

Zhao, R and Pollack, GM (2009) Regional differences in capillary density, perfusion rate, and P-glycoprotein activity: a quantitative analysis of regional drug exposure in the brain. *Biochem Pharmacol* **78**: 1052-1059.

Zoghbi, SS, Liow, JS, Yasuno, F, Hong, J, Tuan, E, Lazarova, N, Gladding, RL, Pike, VW and Innis, RB (2008) ¹¹C-loperamide and its N-desmethyl radiometabolite are avid substrates for brain permeability-glycoprotein efflux. *J Nucl Med* **49**: 649-656.

Footnotes

The work was supported by the United States National Institutes of Health, National Institute of General Medicine [Grant R01 GM60346]; the National Cancer Institute [Cancer Center Support Grant P30 CA21765]; and the American Lebanese Syrian Associated Charities (ALSAC).

Send reprint requests to: Erin G. Schuetz, St Jude Children's Research Hospital, Dept. Pharmaceutical Sciences, 262 Danny Thomas Place, Memphis, TN 38105. Email: erin.schuetz@stjude.org.

Legends for Figures

Figure 1. ***MDR1-luc* transgene.** (A) Map of the *Mdr1-luc* transgene. (B) FISH analysis of heterozygous *MDR1-luc* mouse lung fibroblast metaphase chromosomes with the *MDR1-luc* transgene probe (green) and a biotinylated chromosome 3 centromere specific probe (red) localizing the *MDR1-luc* transgene insertion to band 3A to 3B on chromosome 3.

Figure 2. **Induction of *MDR1-luc* in the head and spinal region of reporter mice by TCPOBOP.** *MDR1-luc* mice were treated daily with TCPOBOP and bioluminescence images were captured ventrally and dorsally 24 hrs after each dose on four consecutive days. Red indicates the highest expression of *MDR1-luc* in each image.

Figure 3. **Induction of *MDR1-luc* by PXR, CAR and GCR agonists in reporter mice, and enhanced bioluminescence by elacridar.** Mice received intraperitoneal injections of vehicle (water), dexamethasone (DEX) or phenobarbital (PB) for 5 hrs. Some mice also received oral gavage of elacridar (ECD) for 4 hrs. Luciferase activity was optically measured *in vivo* at baseline and after drug treatment. Fold induction represents the change in photons in the brain region collected after 5 hrs of drug treatment divided by the photons at time zero in the same animals and is the mean value of four animals/group.

Figure 4. ***Ex vivo* analysis of brains from *MDR1-luc* mice treated with inducers.**

Mice received intraperitoneal injections of dexamethasone (DEX), phenobarbital (PB), or

rifampicin (RIF) for 5 hrs or every 24 hrs for two consecutive days. Some mice also received oral gavage of elacridar (ECD) for the last 4 hrs. Mice were injected with luciferin, brains were removed, placed in luciferin solution, and bioluminescence optically imaged from the dorsal or ventral plane or in brain sagittal sections.

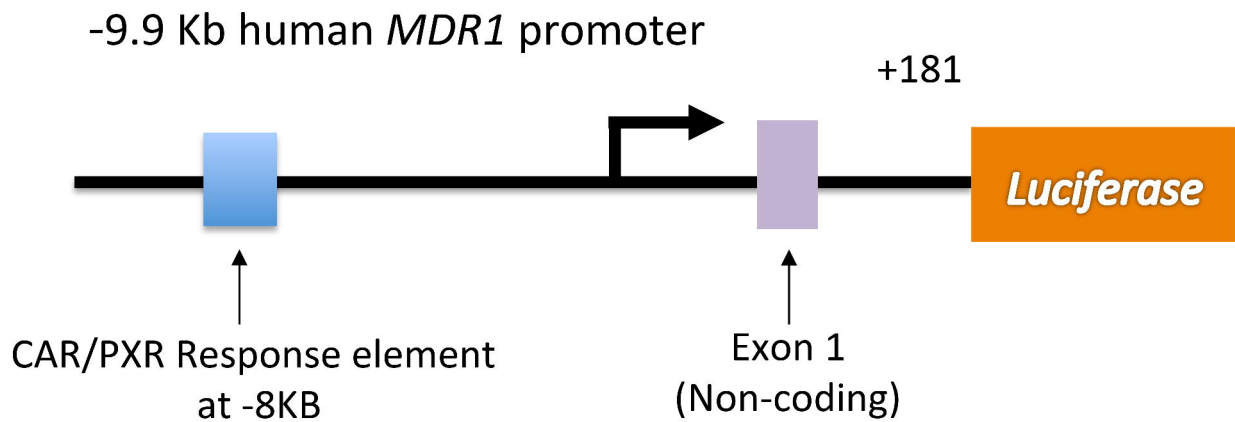
Figure 5. ***Ex vivo* analysis of brains from *MDR1-luc* mice treated with inducers shows regional differences in transcriptional activity.** Mice were treated with drugs as indicted in Fig. 4 legend or rifampicin (RIF) every 24 hrs for four consecutive days, injected with luciferin, brains were immediately removed, sliced coronally (2 mm thickness), placed in a luciferin solution, and bioluminescence imaged. The corresponding brain coronal image from the Allen Brain Atlas (<http://www.brain-map.org>) is included for reference to anatomical regions.

Figure 6. ***Ex vivo* analysis of brains from *MDR1-luc* mice treated with inducers shows regional differences in transcriptional activity.** Mice were treated with phenobarbital for 48 hrs and elacridar as in Fig 4 legend, injected with luciferin, brains were removed, sliced coronally (2 mm thickness), and further microdissected into nine regions (cortex; WT, White matter; STR, Striatum; THM, Thalamus; HP, Hippocampus; SN, Substantia nigra; IC, Internal capsule; CRB, Cerebellum; and BS, Brain Stem). The corresponding brain coronal image from the Allen Brain Atlas is included for reference to anatomical regions.

Figure 7. **Luciferase expression in the brains of *MDR1-luc* mice.** Immunostaining of luciferase (brown) in paraffin sections from the brains of FVB control mice and *MDR1-luc* mice treated with vehicle (control) or phenobarbital (PB) + elacridar as described in Fig. 5 legend and images captured at 63X. Luciferase immunostaining in the BBB is shown.

Figure 8. **Regional heterogeneity in mouse brain Pgp expression and capillary density.** (A) *MDR1-luc* mouse brains were analyzed by dual fluorescent immunohistochemistry for *mouse* Pgp and CD31, the fluorescent signals were quantitated, and the mean intensity of Pgp normalized to CD31 in frontal cortex (FC) and cerebellum (CB). Box plots indicate second and third quartiles. The bold line within the box represents median and whiskers represent the range after excluding the outliers. (B) Fluorescent immunostaining of BBB Pgp in C57BL/6 mouse brain in cortex and cerebellum.

A.



B.

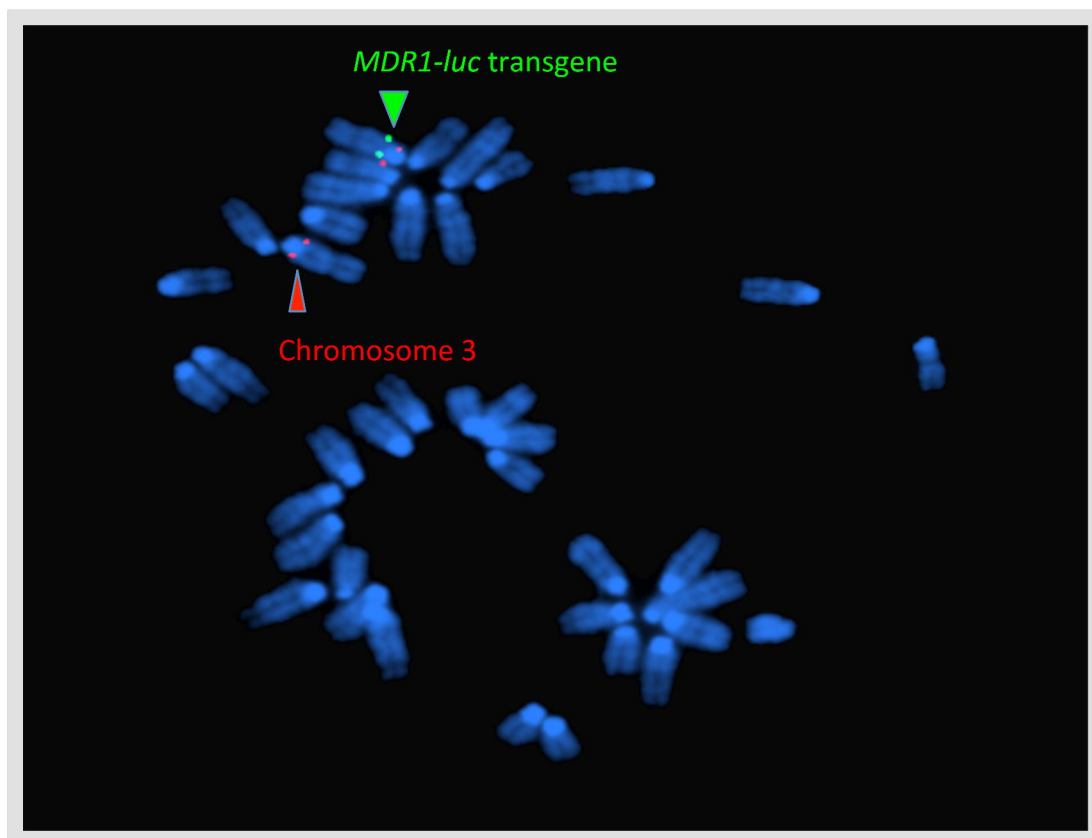


Fig. 1

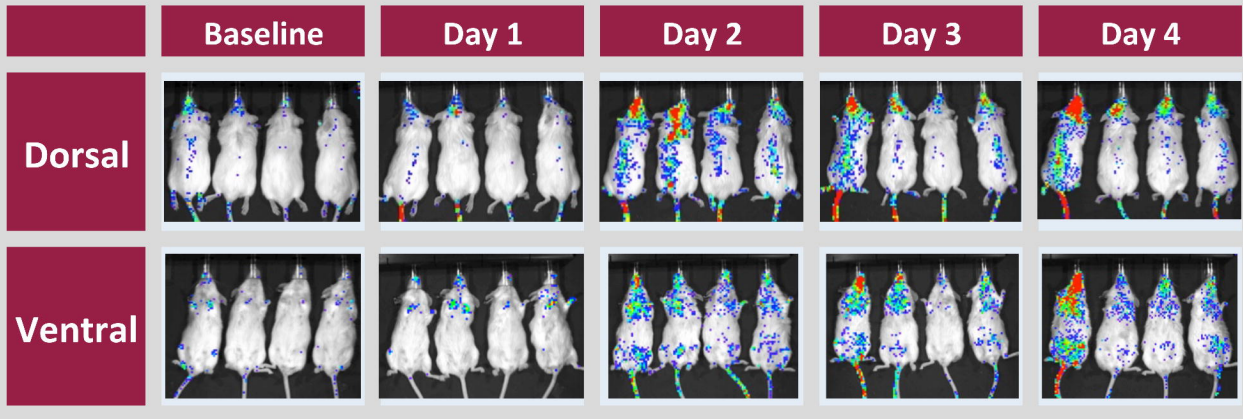


Fig. 2

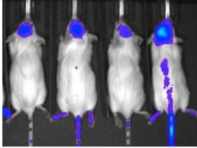
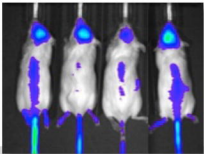
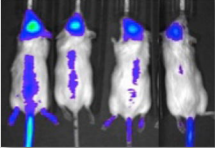
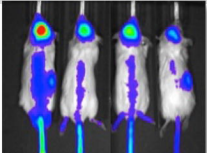
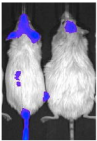
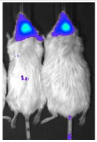
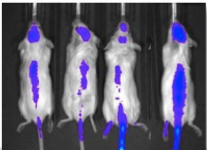
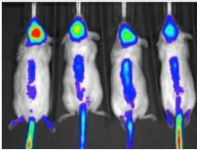
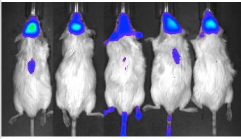
	Treatment	Fold induction
Water 200μl i.p.		x1.00
ECD 4hrs 100mg/kg Oral		x1.47
PB 48hrs 40mg/kg i.p.		x1.37
PB 48hrs 40mg/kg i.p. + ECD		x3.74
DEX 72hrs 5mg/kg i.p.		x1.19
DEX 72hrs 5mg/kg i.p. + ECD		x1.86
DEX 48hrs 200mg/kg i.p.		x1.24
DEX 48hrs 200mg/kg i.p. + ECD		x2.31
RIF 96hrs 50mg/kg i.p.		x1.63

Fig. 3

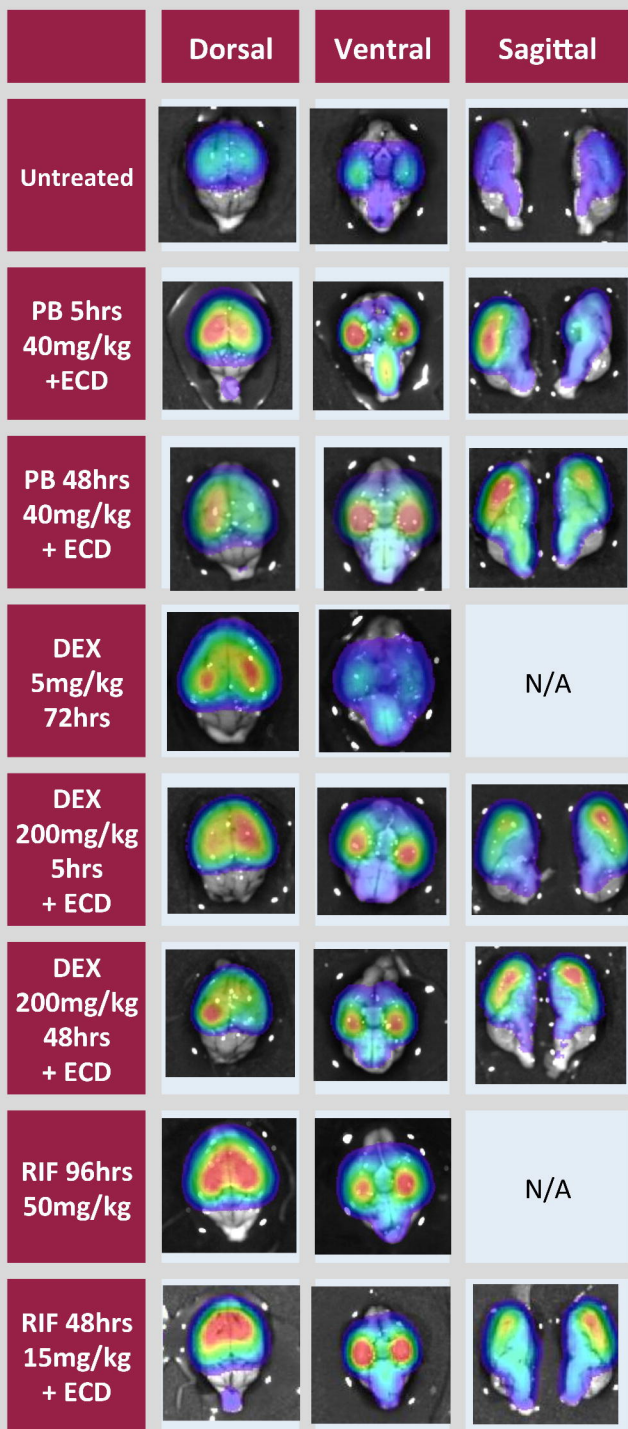
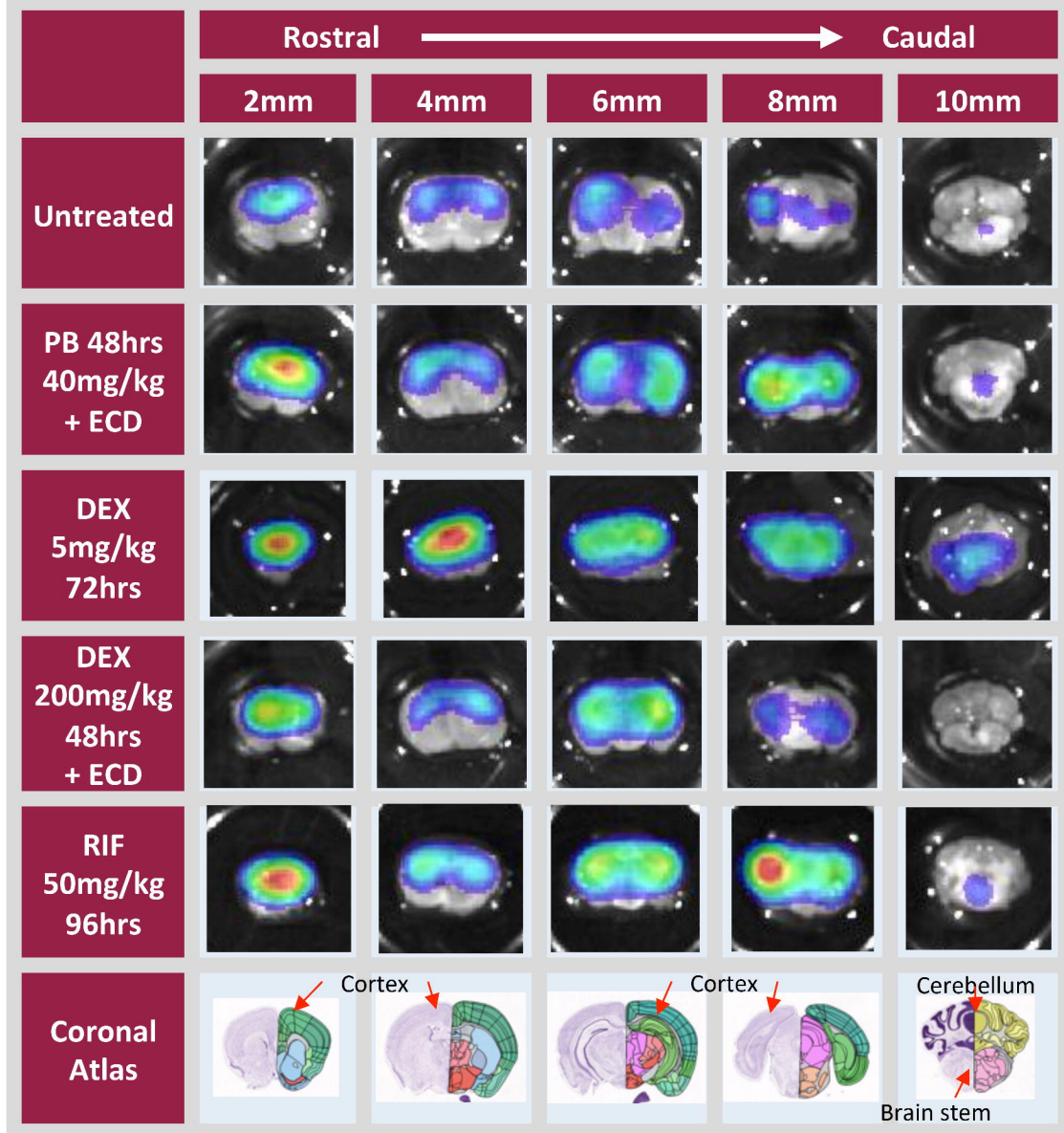


Fig. 4



0 2 4 6 8 10 12 (mm)

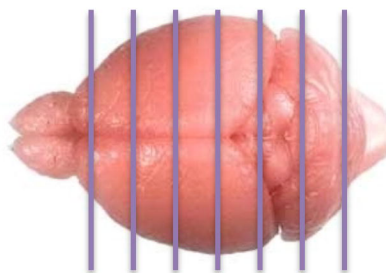


Fig. 5

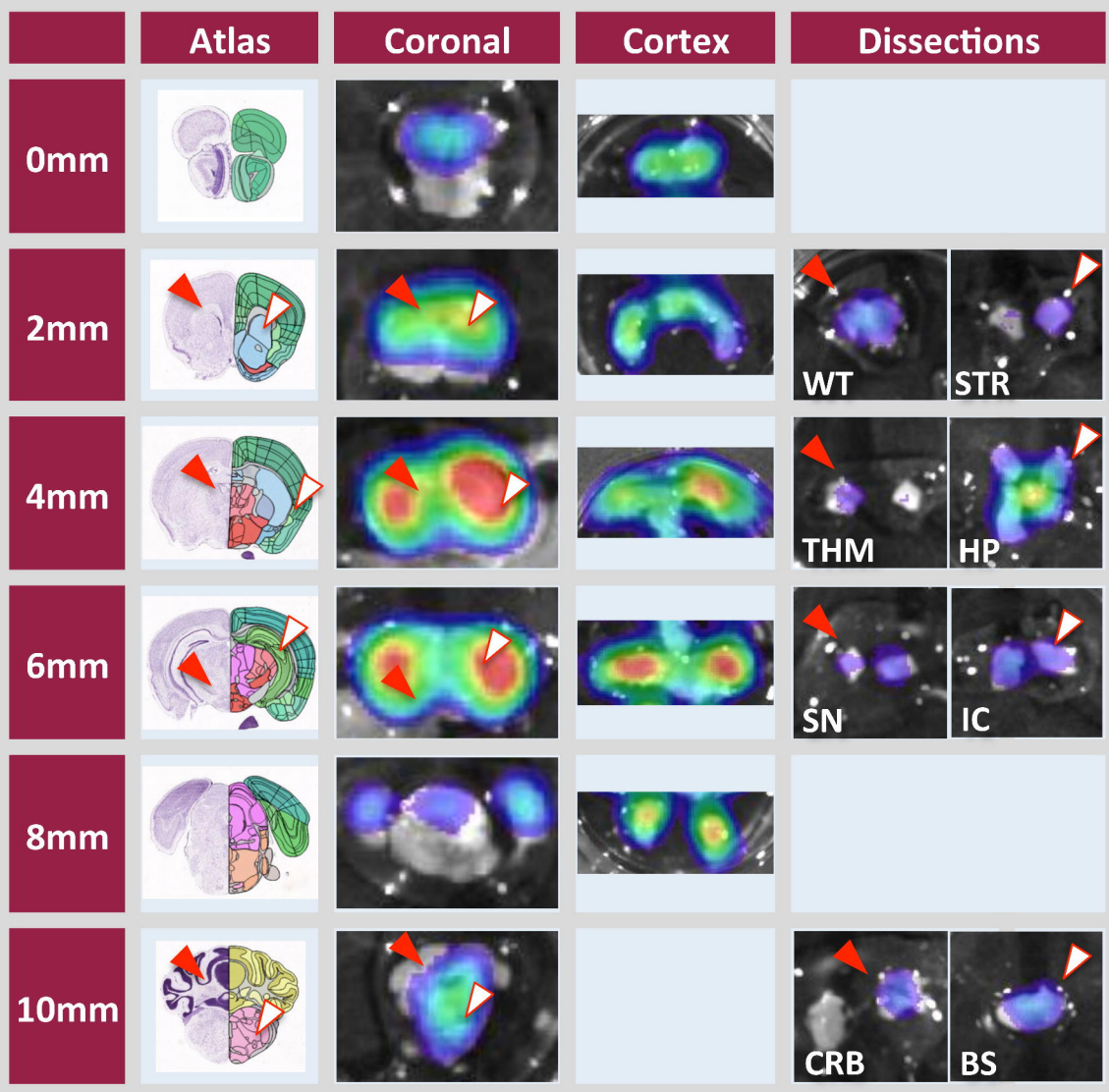


Fig. 6

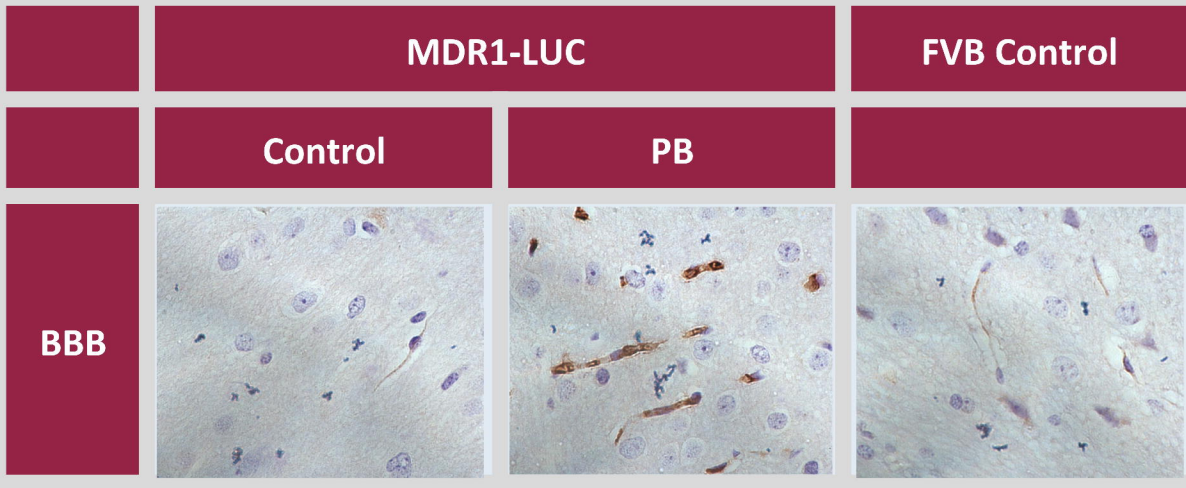
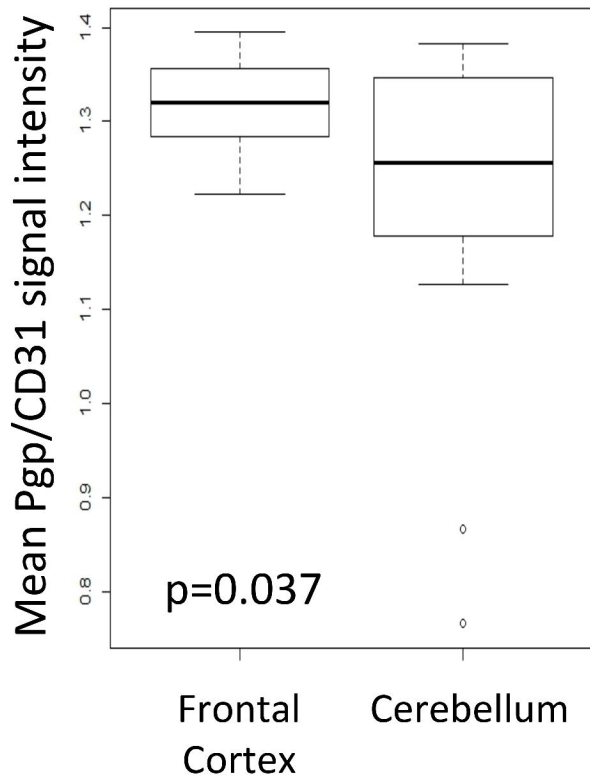


Fig. 7

A.



B.

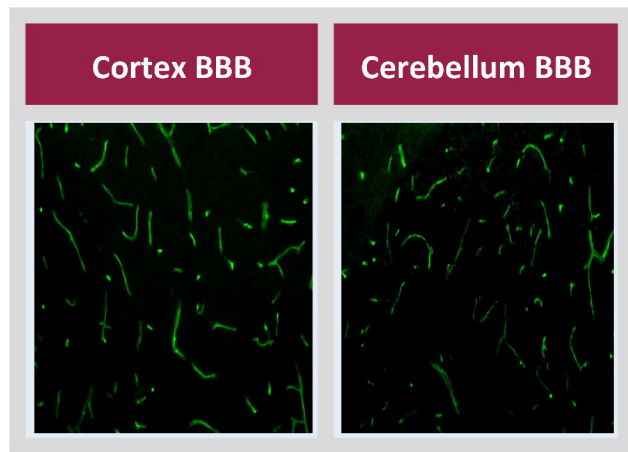


Fig. 8